photonics

MDPI

Article

Performances of PMMA-Based Optical Fiber Bragg Grating Sensor in Extended Temperature Range

Wei Zhang [1,2,*] and David J. Webb [3]

[1] School of Aerospace, Transport, and Manufacturing, Cranfield University, Cranfield MK43 0AL, UK
[2] School of Optoelectronic Engineering, Qilu University of Technology, Jinan 250353, China
[3] Aston Institute of Photonic Technology, Aston University, Birmingham B4 7ET, UK; d.j.webbl@aston.ac.uk
* Correspondence: zhang.wei@cranfield.ac.uk

Abstract: PMMA based optical fiber Bragg grating (POFBG) sensors are investigated in an environmental chamber with controlled temperature and relative humidity at temperature extended to 70 °C. At below a critical temperature of 50 °C the POFBG sensor exhibits good linearity and sensitivity for both temperature and humidity sensing. Nonlinear responses are observed at higher temperature, giving rise to varying, reduced magnitudes of sensitivities. An important feature of POFBG humidity sensing is observed at above critical temperature where the POFBG humidity sensitivity turns from positive to negative. A theoretical model based on Lorentz–Lorenz equation is presented to estimate the dependence of POFBG refractive index on temperature and relative humidity. The experimental results qualitatively agree with the theoretical analyses.

Keywords: fiber Bragg gratings; polymer optical fiber; thermo-optic effect; refractive index humidity dependence

Citation: Zhang, W.; Webb, D.J. Performances of PMMA-Based Optical Fiber Bragg Grating Sensor in Extended Temperature Range. *Photonics* **2021**, *8*, 180. https://doi.org/10.3390/photonics8060180

Academic Editor: Carlos Marques

Received: 11 May 2021
Accepted: 21 May 2021
Published: 23 May 2021

1. Introduction

Polymer optical fibers (POFs) are made of low-cost plastic materials, for example, PMMA. Since POFs are considered as having high optical attenuation compared to their silica counterpart, they have long been overshadowed by the success of silica optical fibers. Recent technological advancements have made POF networks competitive over a range of important applications for short-distance data communication [1]. The physical and chemical properties of polymeric materials are rather different to silica, potentially making them attractive for researchers to exploit in device and sensing applications. Bragg gratings have been inscribed into step index and microstructured POF based on PMMA. The interesting features of POFBGs include the negative refractive index (RI) change against temperature rise and affinity for water that leads to a swelling of the fiber and an increase of RI. The former feature offers a well-conditioned performance for overcoming the cross-sensitivity issues existing in silica fiber while the latter feature leads to a humidity sensor in which the Bragg wavelength of a POFBG increases with humidity [2]. POFBG has been successfully used as a humidity sensor and as a moisture sensor [3,4]. This is a potentially very useful property, which has possible applications in the chemical processing, agricultural, food storage, paper manufacturing, semiconductor, and pharmaceutical industries [5].

POFBG sensors generally operate at around room temperature. POFs may suffer undesirable changes in their optical, thermal, and mechanical properties when aging under high temperature. Note that the high temperature here is only referred to polymer material performance. Conventional PMMA POFs are typically working up to 85 °C [6]. There has been no report on POFBGs operating up to that temperature. In this work we investigate POFBG sensor performance in an extended temperature range in both experiment and theory.

2. Experiments

All the POFBGs used in the work are made of PMMA based step index optical fiber. Before grating fabrication, the POF was annealed in an oven at 80 °C over 7 h. POFBGs mentioned hereafter operate in the 1.5 µm region. These POFBGs are usually UV-glued to a silica optical fiber lead to avoid the high optical loss in the polymer optical fiber [5]. The POFBG used in the experiments is fabricated by attaching a 10 cm length of PMMA optical fiber to a single mode silica fiber down-lead using UV curable glue (AT9390, NTT). This UV glue has a transition temperature of 121 °C, which is close to the PMMA transition temperature. Although connectorized POFBG has been proposed [7], the POFs we used in the experiments are lab-made with considerably varying diameters [8], which makes it not suitable to be connectorized with standard single mode silica optical fiber for practical application. The UV-gluing technique thus was used to achieve stable operation. The PMMA-based POF contained a 5 mm long FBG, fabricated by illuminating from above a phase mask placed on top of the POF using 325 nm UV light from a HeCd laser.

In the experiments, the POFBGs were placed inside an environmental chamber (Sanyo Gallenkamp) to operate at the desired temperature and humidity. They were illuminated via a fiber circulator with light from a broadband light source (Thorlab ASE730) and observed in reflection using an IBSEN I-MON 400 wavelength interrogation system, as shown in Figure 1.

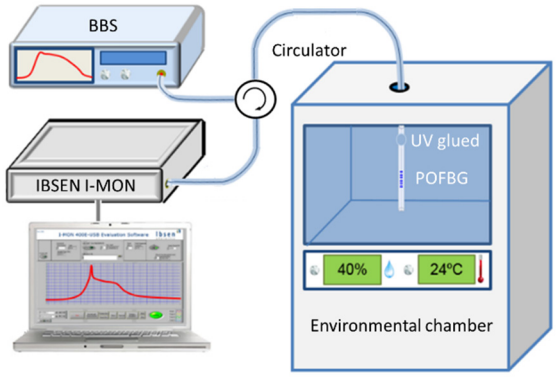

Figure 1. Experimental setup used in this work.

POFBG Wavelength Responses in Extended Temperature Range

For a specific temperature/humidity, the Bragg wavelength change of a POFBG against humidity/temperature change can be expressed as [9]

$$\begin{aligned} \Delta\lambda_B &= \lambda_B(\eta + \beta)\Delta H \\ \Delta\lambda_B &= \lambda_B(\alpha + \xi)\Delta T \end{aligned} \quad (1)$$

where λ_B is the initial Bragg wavelength, η is the normalized refractive index (RI) change with humidity, β is the swelling coefficient related to humidity induced volumetric change, α is the thermal expansion coefficient (TEC), and ξ is the thermo-optic coefficient. From (1), one can see that there are two factors contributing to the wavelength change of a POFBG. One is the RI change induced. The other is the length change of the PMMA-based fiber.

It has been reported [10] that solid drawn polymers and stretched elastomers exhibit anisotropic expansion, which mainly depends on the polymer processing history. It was also noticed that rising temperature releases the residual drawing stress in the fiber, leading to fiber shrinkage, thus causing an additional negative change of the POFBG wavelength [11,12]. Annealing POFs can mitigate this issue. However, it has been reported that the usual annealing process is far from enough [12,13]. This consequently gives rise to inconsistent POFBG sensor performance [4].

An experiment was designed to examine the performance of the POFBG sensor. A pre-strain technique was used to eliminate the residual stress related inconsistency [14,15],

in which the POFBG was strained using a translation stage and then glued to an INVAR bar. The device length change due to changing temperature in this case is not determined by the POF thermal expansion but by INVAR thermal expansion (the influence of the glue is negligible as the glued points are very small in size compared to the POF length). In addition, the fiber cannot lengthen in the longitudinal direction, but there can remain a deformation in the transverse plane. This consequently leads to the change of refractive index of the fiber which can be estimated by using the Lorentz–Lorenz relation [16]. This change is insignificant due to the small ratio of fiber core diameter to fiber length and it is ignored in this work. The pre-strained POFBG was then placed in the environmental chamber for the test of POFBG performance. Since the ends of the POFBG were fixed, the length of the PMMA optical fiber between the two clamping points does not vary with either temperature or humidity (given that the applied strain was larger than any temperature/humidity induced fiber length change). In this case, the POFBG temperature/humidity sensitivity only relies on the thermo-optic effect/RI humidity dependence of the fiber.

The highest operation temperature for the PMMA based fiber grating sensor, reported so far, was 50 °C [4,16]. POFBG was reportedly heated up to 92 °C [11] in which, however, only the grating section of 5 mm was heated by a power resistor to that nominal temperature with unknown surrounding humidity. In that case the whole POFBG sensor was not considered as operating at that high temperature and the POFBG sensing performance was difficult to verify as the POF shrinkage overwhelms the contributions from refractive index change and fiber thermal expansion.

With the POFBG being pre-strained to 8000 με we first investigated the POFBG humidity performance at the temperatures of 25, 35 and 45 °C, respectively. At each temperature the relative humidity of the environmental chamber was programmed to change with a step of 10% RH. The captured POFBG wavelength responses are shown in Figure 2.

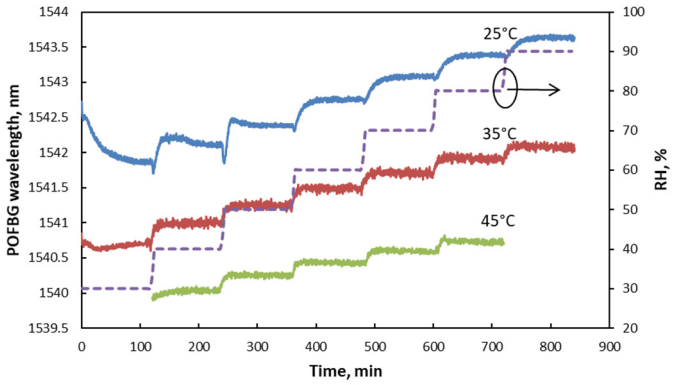

Figure 2. Measured POFBG humidity responses at 25, 35 and 45 °C.

Further experiments were carried out at higher temperature. The POFBG wavelength was monitored with the chamber temperature set to 50 °C while the relative humidity was programmed to vary from 20 to 80% RH with a step increment of 20% RH. The experiment repeated at the chamber temperature of 55, 60, 65 and 70 °C, respectively. The captured POFBG wavelength responses are shown in Figure 3.

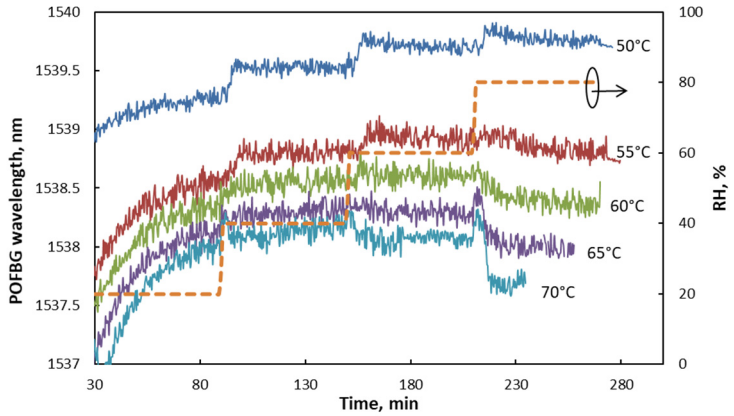

Figure 3. Measured POFBG humidity responses at 50 °C and above.

3. Results

3.1. POFBG Humidity Sensitivity

From Figure 2 one can see that the POFBG exhibits good response against humidity change while it also shows a tendency of reduced humidity sensitivity with temperature increase. The POFBG responses in Figure 3 look noisy and do not show as clear a tendency as those in Figure 2. The noisy responses mainly arise from the strained fiber grating which was picking up the chamber vibration during the experiments. The vibration becomes stronger when the chamber operates at higher temperature. The stabilized POFBG wavelengths at each humidity level are summarized in Figure 4.

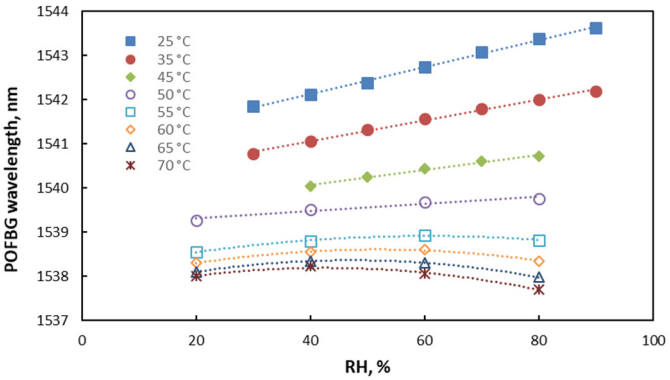

Figure 4. POFBG wavelengths against humidity change at different temperatures.

One can see that the first 3 sets of data show very good linear relationship between the POFBG wavelength and humidity change, giving a humidity sensitivity of 31 pm/% RH at 25 °C, 23 pm/% RH at 35 °C and 17 pm/%RH at 45 °C, respectively. These sensitivities agree with those reported in [4]. The POFBG response at 50 °C shows a greatly reduced sensitivity of 8 pm/% RH.

From 55 °C on the POFBG responses show clear nonlinearity against humidity change. At 55 °C the POFBG response reach the maxima at around 50% RH. At higher temperatures the POFBG humidity sensitivity turns negative at the relative humidity even lower than 50% RH. This feature of POFBG sensor has never been observed before.

3.2. POFBG Temperature Sensitivity

The POFBG responses are summarized to show the temperature sensing performance at different relative humidities, as shown in Figure 5. At a temperature below 50 °C the POFBF sensor exhibits good linear response against temperature at different relative humidities. In this linear region the POFBG temperature sensitivity is calculated as −104 pm/°C at 40% RH, −116 pm/°C at 60% RH, and −133 pm/°C at 80% RH. These

sensitivities are roughly two-thirds of the calculated values based on the thermo-optic coefficients of PMMA at the same relative humidity, due to the restricted expansion in the fiber length direction, and in agreement with those reported in [14]. It can be seen that for temperature sensing the POFBG exhibits strong nonlinearity at temperatures above 50 °C with reduced magnitude of temperature sensitivity.

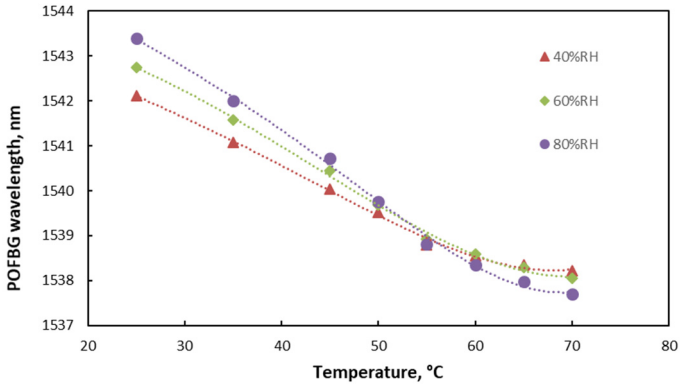

Figure 5. POFBG wavelengths against temperature change at different humidity levels.

3.3. Analysis of POFBG Sensing Performance

As aforementioned, in this work a pre-strain of 8000 με was applied to the POFBG sensor to overcome inconsistent POFBG sensor performance induced by residual drawing stress. This pre-strain is supposed to be larger than any temperature/humidity induced fiber expansion so only refractive index change induced by temperature/humidity makes a contribution to the POFBG wavelength change. The POFBG was pre-strained at the room condition of ~50% RH and 25 °C. The thermal expansion and the humidity induced length change of POFBG can be estimated based on the property of bulk PMMA. The TEC of bulk PMMA is the function of both temperature and humidity and is estimated as 70×10^{-6}/°C at dry condition, 25 °C to 115×10^{-6}/°C at 90%RH, 70 °C [17,18]. The humidity induced length change is temperature independent [19] and the change rate estimated as 0.114% at 50%RH to 0.236% at 80%RH. This ensures the temperature/humidity induced fiber expansion does not exceed the pre-strain. On this condition one may analyze the POFBG performance by looking into the refractive index change of PMMA against temperature and humidity. It should be noted that the detailed composition of dopant and copolymer used in a specific PMMA-based optical fiber is often not known. POFBG performance can be approximated by that of pure PMMA, as the amount of dopant is very small.

The refractive index of a substance can be defined by Lorentz–Lorenz equation. It allows the refractive index to be obtained on the molar refraction which is often represented as the sum of the refractions of certain constituents [20]. The refractive index n of a polymer with moisture concentration C_m is expressed as [21],

$$\frac{n^2-1}{n^2+2} = k_p\rho_p + \left(1 - \frac{f}{f_c}\right)k_m C_m \tag{2}$$

where f is the fraction of the absorbed moisture that contributes to an increase in polymer volume, f_c is the critical value associated with the properties of moisture and polymer, $C_m = S \cdot H$, the moisture mass in the unit volume of the polymer including moisture, S is the moisture solubility of the polymer; ρ_i and k_i ($i = p$, m, representing polymer, moisture) are the density and the specific refraction which is the molar refraction divided by the molecular weight, respectively.

According to [22], ρ_p, the polymer density, is a function of moisture absorbed by PMMA, proportional to relative humidity H. For bulk PMMA, f increases with temperature and f_c is constant over temperature ($f = f_c$ at the critical temperature of 50 °C) [21]. Specific refraction, k_i, generally is calculated from the measurement of refractive index [23],

which implies that k_i is a function of temperature and humidity. In reference [21] k_i is considered constant by introducing the factor $(1 - f/f_c)$ in order to simplify the mathematical processing. The term S weakly depends on temperature in a form of e^{-kT} where k is Boltzmann's constant [24]. We will use this simplification to qualitatively analyze the POFBG performance.

The properties of POFBG that appeared in (2) are summarized as,

- ρ_p, the polymer density, is a linear function of moisture;
- f $(0 \leq f \leq 1)$ increases with temperature, and $f = f_c$ at the critical temperature of 50 °C;
- k_i, is a weak function of temperature and humidity, approximately constant; and
- S slowly decreases with temperature.

At a constant temperature, the humidity dependence of the refractive index can be derived by differentiating both sides of Equation (2) as a function of H,

$$\frac{dn}{dH} = \frac{(n^2+2)^2}{6n}\left[\left(1 - \frac{f}{f_c}\right)k_m S + k_p \rho_p'\right] \tag{3}$$

There are two terms on the right side of (3). For the temperature below 50 °C, $f < f_c$, both terms are positive and almost constant. The POFBG refractive index is proportional to the humidity. The POFBG humidity responses therefore show good linearity. As shown in Figure 4, from 25 to 45 °C the POFBG responses show good linearity and the humidity sensitivity decreases with temperature.

The first term makes less contribution to the POFBG response at increased temperature because S decreases slowly with temperature and $(1 - f/f_c)$ approaches zero with temperature increasing to 50 °C. This leads to decreased humidity sensitivity. Experimental results show that at 50 °C the humidity sensitivity is small. At a temperature above 50 °C, $f > f_c$, the first term turns negative, further reducing the sensitivity. With temperature and/or humidity increasing, the first term may cancel the second term and the sensitivity turns negative. In Figure 4, at a temperature $\geq$ 50 °C the humidity sensitivity starts small but positive and turns negative with increasing humidity. The dependence of k_i on temperature and humidity becomes more significant at higher temperature as the humidity sensitivity becomes smaller. As a result, the humidity sensitivity at higher temperature exhibits increasing nonlinearity.

To determine the thermo-optic coefficient at a constant RH%, it can be derived by differentiating it as a function of T,

$$\frac{dn}{dT} = \frac{(n^2+2)^2}{6n}\left[\left(1 - \frac{f}{f_c}\right)k_m H S' - \frac{k_m S H}{f_c} f'\right] \tag{4}$$

Note here that both S and f are functions of temperature, and S' and f' are the corresponding derivatives. S slowly decreases with temperature, producing a small, negative S' and f increases with temperature. For a temperature below 50 °C, on the right side of (4) both the first term and the second are negative but the second term dominates. Therefore, in Figure 5, for the temperature below 50 °C the temperature responses of the POFBG all exhibit good linearity and the magnitude of temperature sensitivity at higher humidity level is larger.

The first term turns positive as $f > f_c$ after 50 °C and cancels part of the contribution from the second term. It leads to the reduced magnitude of temperature sensitivity. The experimental results in Figure 5 show smaller magnitude of temperature sensitivity and more nonlinearity after 50 °C as the contribution of k_i becomes more significant.

In Figure 5 the curves representing the POFBG temperature responses at different humidity levels cross at different temperatures above 50 °C. This is slightly different from the case for bulk PMMA [21], in which the temperature responses of PMMA refractive index cross at 50 °C, in coincidence with the critical temperature. Since the detailed figures

of some parameters in (3) and (4) are not available, it is difficult to determine if this disagreement is real or distorted due to the experimental error.

There also exists some disagreement between the POFBG temperature sensing performance and the temperature dependence of the bulk PMMA refractive index in [21]: the magnitude of the measured thermo-optic coefficient of bulk PMMA increases above the critical temperature; in contrast, the POFBG responses exhibit reduced magnitude of sensitivity above the critical temperature. The similar responses to the bulk PMMA were observed in POFBGs [25], which were verified as caused by residual drawing stress. Residual drawing stress exists in both bulk PMMA and POF [10,12]. By using pre-strained POFBG one can eliminate the effect of residual drawing stress in the POFBG wavelength response. This may indicate that the effect of residual drawing stress should be considered when looking into the thermo-optic coefficient in bulk PMMA.

4. Conclusions

The POFBG sensing performances have been investigated in the extended temperature range. At below a critical temperature of ~50 °C the POFBG sensor shows good linear responses and considerable sensitivities. Above the critical temperature both POFBG humidity and temperature responses exhibit nonlinearity. The POFBG humidity sensitivity could turn from positive to negative above the critical temperature. A simplified theoretical model based on Lorentz–Lorenz equation was used to qualitatively analyze the POFBG sensing responses and shows good agreement with the experimental results.

When the POFBG sensor operates below the critical temperature both humidity and temperature responses show good linearity. The general expression of POFBG responses can be obtained in order to facilitate the POFBG sensing applications. However, the POFBG sensor exhibits negative humidity sensitivity above the critical temperature. This means that ambiguity could be introduced when POFBG is used for humidity sensing above the critical temperature. This ambiguity would restrict the POFBG humidity sensor from certain applications where the environment temperature is high. On other hand, the POFBG humidity negative sensitivity may be introduced in some special applications.

Author Contributions: Conceptualization, W.Z. and D.J.W.; methodology, W.Z.; formal analysis, W.Z.; investigation, W.Z.; writing—original draft preparation, W.Z.; writing—review and editing, W.Z. and D.J.W.; project administration, D.J.W. Both authors have read and agreed to the published version of the manuscript.

Funding: This research received no external funding.

Institutional Review Board Statement: Not applicable.

Informed Consent Statement: Not applicable.

Data Availability Statement: Not applicable.

Conflicts of Interest: The authors declare no conflict of interest.

References

1. Polishuk, P. Plastic optical fibers branch out. *IEEE Commun. Mag.* **2006**, *44*, 140–148. [CrossRef]
2. Zhang, C.; Zhang, W.; Webb, D.J.; Peng, G.-D. Optical fiber temperature and humidity sensor. *Electron. Lett.* **2010**, *46*, 643. [CrossRef]
3. Zhang, W.; Webb, D.J.; Lao, L.; Hammond, D.; Carpenter, M.; Williams, C. Water content detection in aviation fuel by using PMMA based optical fiber grating. *Sens. Actuators B Chem.* **2019**, *282*, 774–779. [CrossRef]
4. Zhang, W.; Webb, D.J. Humidity responsivity of poly(methyl methacrylate)-based optical fiber Bragg grating sensors. *Opt. Lett.* **2014**, *39*, 3026–3029. [CrossRef] [PubMed]
5. Webb, D.J.; Kalli, K. Polymer fiber Bragg gratings. In *Fiber Bragg Grating Sensors: Thirty Years from Research to Market*; Cusano, A., Cutolo, A., Albert, J., Eds.; Bentham Science Publishers Ltd.: New York, NY, USA, 2010.
6. Peng, G.-D. *Handbook of Optical Fibers*; Springer Nature Singapore Pte Ltd.: Singapore, 2019.
7. Abang, A.; Webb, D.J. Demountable connection for polymer optical fiber grating sensors. *Opt. Eng.* **2012**, *51*, 080503. [CrossRef]
8. Zhang, W.; Webb, D.J.; Peng, G.-D. Investigation into time response of polymer fibre Bragg grating based humidity sensors. *IEEE J. Lightwave Technol.* **2012**, *30*, 1090–1096. [CrossRef]

9. Zhang, W.; Webb, D.J. General Expression of Poly(Methyl Methacrylate) Optical Fiber Bragg Grating Sensing Response. *IEEE Photonics Technol. Lett.* **2019**, *31*, 234–237. [CrossRef]
10. Salem; David, R. *Structure Formation in Polymeric Fibers*; Hanser-Gardner Publications: Cincinnati, OH, USA, 2001.
11. Carroll, K.E.; Zhang, C.; Webb, D.J.; Kalli, K.; Argyros, A.; Large, M.C.J. Thermal response of Bragg gratings in PMMA mi-crostructured optical fibers. *Opt. Express* **2007**, *15*, 8844–8850. [CrossRef] [PubMed]
12. Stajanca, P.; Cetinkaya, O.; Schukar, M.; Mergo, P.; Webb, D.J.; Krebber, K. Molecular alignment relaxation in polymer optical fibers for sensing applications. *Opt. Fiber Technol.* **2016**, *28*, 11–17. [CrossRef]
13. Ishigure, T.; Hirai, M.; Sato, M.; Koike, Y. Graded-Index Plastic Optical Fiber with High Mechanical Properties Enabling Easy Network Installations. I. *J. Appl. Polym. Sci.* **2004**, *91*, 404–409. [CrossRef]
14. Zhang, W.; Webb, D.J.; Peng, G.-D. Enhancing the sensitivity of poly(methyl methacrylate) based optical fiber Bragg grating temperature sensors. *Opt. Lett.* **2015**, *40*, 4046–4049. [CrossRef] [PubMed]
15. Woyessaa, G.; Pedersen, J.K.M.; Nielsenc, K.; Bang, O. Enhanced pressure and thermal sensitivity of polymer optical fiber Bragg grating sensors. *Opt. Laser Technol.* **2020**, *130*, 106357. [CrossRef]
16. Prod'Homme, L. A new approach to the thermal change in the refractive index of glasses. *Phys. Chem. Glasses* **1960**, *1*, 119–122.
17. Waxler, R.M.; Horowitz, D.; Feldman, A. Optical and physical parameters of Plexiglas 55 and Lexan. *Appl. Opt.* **1979**, *18*, 101–104. [CrossRef] [PubMed]
18. Startsev, O.V.; Rudnev, V.P. Reversible moisture effects in the climatic ageing of organic glass. *Polym. Degrad. Stab.* **1993**, *39*, 373–379. [CrossRef]
19. Thomas, A.M. Moisture permeability, diffusion and sorption in organic film-forming materials. *J. Appl. Chem.* **1951**, *1*, 141–158. [CrossRef]
20. Liu, Y.; Daum, P.H. Relationship of refractive index to mass density and self-consistency of mixing rules for multicomponent mixtures like ambient aerosols. *Aerosol Sci.* **2008**, *39*, 974–986. [CrossRef]
21. Watanabe, T.; Ooba, N.; Hida, Y.; Hikita, M. Influence of humidity on refractive index of polymers for optical waveguide and its temperature dependence. *Appl. Phys. Lett.* **1998**, *72*, 1533. [CrossRef]
22. Turner, D.T. Polymethyl methacrylate plus water: Sorption kinetics and volumetric changes. *Polymer* **1982**, *23*, 197–202. [CrossRef]
23. Patel, M.P.; Davy, K.W.M.; Braden, M. Refractive index and molar refraction of methacrylate monomers and polymers. *Biomaterials* **1992**, *13*, 643–645. [CrossRef]
24. Fan, X. Mechanics of Moisture for Polymers: Fundamental Concepts and Model Study. In Proceedings of the 9th International Conference on Thermal, Mechanical and Multiphysics Simulation and Experiments in Micro-Electronics and Micro-Systems, EuroSimE 2008, Freiburg im Breisgau, Germany, 20–23 April 2008.
25. Zhang, W.; Webb, D.J. *Factors Influencing the Temperature Sensitivity of PMMA Based Optical Fiber Bragg Gratings*; Photonics Europe: Brussels, Belgium, 2014.

Performances of PMMA-based optical fiber bragg grating sensor in extended temperature range

Zhang, Wei

2021-05-23

Zhang W, Webb DJ. (2021) Performances of PMMA-based optical fiber bragg grating sensor in extended temperature range. Photonics, Volume 8, Issue 6, June 2021, Article number 180
https://doi.org/10.3390/photonics8060180